The Interfacial Reaction of Modified Poly(arylether sulfone)s and Polyaramides

DIETMAR MÄDER,[1] MARTINE COLLAUD COEN,[1] JÖRG KRESSLER,[1] ROLF MÜLHAUPT,[1] MARTIN WEBER[2]

[1] Albert-Ludwigs-Universität Freiburg, Institut für Makromolekulare Chemie und Freiburger Materialforschungszentrum, Stefan-Meier-Strasse 21, D-79104 Freiburg i. Br., Germany

[2] BASF AG, Kunststofflaboratorium, D-67056 Ludwigshafen, Germany

Received 17 October 1996; accepted 20 November 1996

ABSTRACT: It is shown that a fracture test using an asymmetric double cantilever beam test geometry is a powerful tool to study the effect of interfacial reactions on the improvement of the interfacial fracture toughness (G_c) of immiscible polymer systems. The G_c values between a partially aromatic polyamide (PA) and a poly(arylether sulfone) (PSU) can be increased significantly when reactive PSUs are used which are obtained by grafting with maleic anhydride by introducing pyromellitic anhydride end-groups or by introducing carboxylic acid groups via copolymerization. Optical and atomic force microscopy investigations of the fracture surfaces show different failure mechanisms for weak and strong interfaces. For weak interfaces it was possible to determine the crack opening geometry using interference microscopy. For significantly reinforced interfaces rib marking lines on the PSU fracture surface can be observed. X-ray photoelectron spectroscopy (XPS) measurements reveal that with increasing toughness of the interface more and more cohesive failure of the PA occurs. This results in an increasing amount of nitrogen detected on the PSU fracture surface and simultaneously no sulfur is detected on the PA fracture surface. © 1997 John Wiley & Sons, Inc. J Appl Polym Sci **65:** 567–579, 1997

INTRODUCTION

Recently the combination of engineering plastics with different application profiles has become more and more popular for several reasons.[1] Blending of different engineering materials may increase their range of potential applications by achieving synergistic effects leading to improved mechanical, electrical, or thermal properties. Engineering plastics, e.g., polysulfones, poly(arylether sulfone)s, polyimides, and poly(ether ether ketone)s, are relatively expensive and their application is rather limited for specialties. Blending may broaden the spectrum of application for these polymers substantially. Because of the frequent, highly incompatible character of the blends, it is necessary to improve the strength of very weak interfaces. Several methods to promote interfacial adhesion have been proposed, such as using preformed block or graft copolymers[2] and random copolymers, respectively.[3] But the most efficient way to increase the interfacial strength is reactive blending.[4] Here the formation of block copolymers, graft copolymers, or networks occurs directly at the interface during reactive blending or processing.

This study deals with the interfacial reaction of modified poly(arylether sulfones) (PSU) with a partially aromatic polyamide (PA). Both polymers are engineering plastics and have their special application profiles. PA is a semicrystalline polymer with a melting point of 295°C and a glass transition temperature, T_g, of 100°C. PSU is a complete amorphous polymer and has a T_g of

Correspondence to: Jörg Kressler.
 CCC 0021-8995/97/030567-13

187°C. Blending of both polymers might result in new material properties. Because of the highly incompatible character of both polymers, it is necessary to compatibilize them. Therefore, the PSU, which is a condensation product of bisphenol A and dichlorodiphenylsulfone (DCDPS), is modified by grafting with maleic anhydride, by copolymerization with 4,4-bis(4′-hydroxyphenyl)valeric acid, commonly known as diphenolic acid (DPA), or by introducing pyromellitic anhydride endgroups. The carboxylic acid or anhydride groups are able to react with the amine groups of the polyamide, which is a condensation product of hexamethylenediamine, terephthalic acid, and ϵ-caprolactam. The fracture toughness is measured by an asymmetric double cantilever beam (ADCB) test[5] of multilayer specimens in order to study the efficiency of the interfacial reactions. Microscopic techniques such as light microscopy (LM) and atomic force microscopy (AFM) are employed to study the fracture mechanisms. Finally, X-ray photoelectron spectroscopy (XPS) is used for a quantitative analysis of the chemical composition of the fracture surfaces.

EXPERIMENTAL

Materials

For the reactive blending studies, PSU copolymers with different amounts of diphenolic acid (DPA) were synthesized according to procedures given in the literature.[6–8] Anhydride functionalized PSUs were prepared by either grafting PSU with maleic anhydride[9] or by the reaction of amino-terminated PSU with an excess of pyromellitic dianhydride.[10] DPA, maleic anhydride, bisphenol A, DCDPS, dicumylperoxide, and pyromellitic dianhydride were obtained from Aldrich. *N*-methyl-2-pyrrolidone (NMP) was dried with CaH_2 and distilled.

The nonmodified PSU as well as the PA are commercial products of BASF, Ultrason® S and Ultramid® T, respectively. All characteristic data of the polymers are given in Table I. All functionalized PSUs have a molecular weight well above the entanglement molecular weight of PSU, which is M_e = 2260 g/mol.[11] Because both polymers are commercial products, it is possible to detect small amounts of impurities in both materials. The presence of very small amounts of silicon-containing compounds could be detected at the surface as well as in the bulk phase of both materials by XPS. Very rarely, inorganic impurities such as salts or oxides were detected on the surface of the polymers by scanning electron microscopy coupled with EDX (energy dispersive X-ray analysis).

Synthesis of Poly(arylether sulfone)-g-Maleic Anhydride (PSU-g-MA)

Eighty g of PSU were dissolved in chlorobenzene and the solution was heated to reflux. Eighteen g of maleic anhydride and 5.4 g dicumylperoxide were added over a period of 4 h. After refluxing for another hour the solution was cooled to room temperature and the polymer was isolated by precipitation in ethanol. The polymer was filtered and redissolved in NMP and again precipitated in a mixture of NMP/H_2O (2 : 8). After filtration the polymer was extracted with hot water and dried. Finally, the product was dried at 130°C in vacuum for 12 h. The amount of grafted anhydride units was determined to be 0.4 wt % (equal to 1.8 mol % of repeat units shown in Table I) by potentiometric titration in *N,N*-dimethylformamide.

Synthesis of Poly(arylether sulfones) Containing Diphenolic Acid Units (PSU-COOH$_x$)

DPA, bisphenol A, DCDPS, and K_2CO_3 were dissolved in dry NMP. The mixture was heated to 190°C for 6 h under nitrogen. During this time the azeotropic mixture of NMP and water was continuously removed. The solution was cooled to room temperature, diluted with NMP, and filtered. After this procedure an excess of acetic acid was added to the solution and after further stirring (30 min) the polymer was isolated by precipitation in water. The polymer was extracted three times with hot water and dried for 12 h at 130°C. The amounts of incorporated DPA units (x [mol %]) were estimated using ^{1}H-NMR-spectroscopy (in $CDCl_3/CF_3COOD$ 1 : 1). The ratio of monomer units derived from DPA and bisphenol A was calculated using the signal intensities in the ^{1}H-NMR-spectra, taking into account the signal intensities of the CH_2-groups of DPA (δ = 2.2 ppm and 2.5 ppm) with respect to the signal intensity of the CH_3-groups of the units derived from bisphenol A (δ = 1.6 ppm).

Synthesis of Poly(arylether sulfone) with Pyromellitic Anhydride Endgroups (PSU-t-PyA)

This product was synthesized according to the procedure given by Myers.[10] First amine-termi-

Table I Used Polymers, Their Abbreviations, Structural Units, and Physical Properties

Polymer	Structural Units	T_g/T_m[a] (°C)	M_w[b] (g/mol)	M_w/M_n[b]	VN[c] (mL/g)
Poly(hexamethylenediamine-terephthalic acid-*co*-caprolactam) (PA)[d]	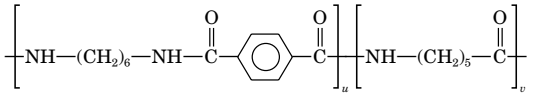	100/295	35,000	2.3	130.0[e]
Poly(oxy-1,4-phenylene-sulfonyl-1,4-phenylenoxy-1,4-phenyleneisopropylidene-1,4-phenylene) (PSU)	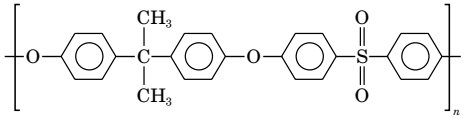	187	30,000	2.5	64.0
(*N*-(*p*-phenyl)-pyromellitic anhydride)-terminated-polysulfone (PSU-t-PyA)	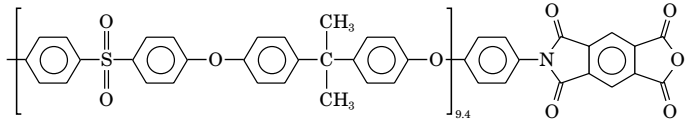	179	13,300	3.0	24.2
Polysulfone with 4,4-bis(4′-hydroxyphenyl) pentanoic acid units (PSU-COOH$_x$)[f]	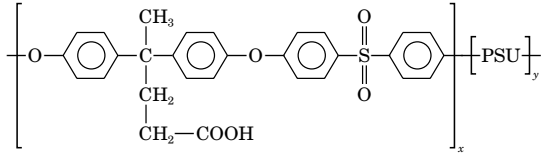	180[g] 179[h] 176[i]	23,000 17,100 10,000	3.1 3.2 2.3	31.2 27.7 18.8
Maleic anhydride-grafted-polysulfone (PSU-g-MA)	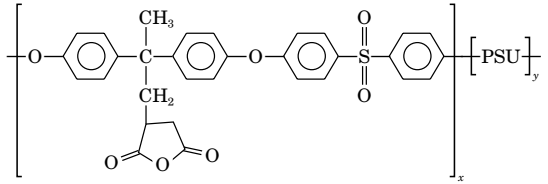	185	42,300	2.2	51.4

[a] The glass transition temperatures of the polymers were determined by DSC measurements (Perkin-Elmer DSC 7) using a heating rate of 10 K/min.
[b] The samples were characterized by GPC measurements in THF solution; molecular weights and molecular weight distributions were estimated based on polystyrene standards using a UV detector. The PA sample is measured after conversion with trifluoroacetic acid.
[c] VN means viscosity number. The viscosity number was measured at a concentration of 1 wt % in NMP at 25°C.
[d] u = 52 mol %, v = 48 mol %.
[e] Measured from a 1 wt % solution in H_2SO_4 (96 wt %).
[f] x means DPA units (in mole percent).
[g] x = 1.7.
[h] x = 4.5.
[i] x = 8.8.

nated PSU was prepared by copolymerization of *p*-aminophenol as endcapping reagent during the condensation of DCDPS and bisphenol A.[12] The amine-terminated PSU and pyromellitic dianhydride were dissolved in NMP and xylene was added to remove formed water as an azeotrope in order to give anhydride end-capped PSU. After reacting at 198°C for 1.5 h the product was isolated by precipitation in methanol. The polymer was extracted three times with hot water and dried for 12 h at 130°C. The amount of pyromellitic anhydride end groups was 10.6 mol % referring to one repeat unit.

Preparation of Joint Specimens

The PSU and the PA pellets were injection-molded into disks of 6 cm in diameter. Thin films of the modified PSUs were prepared by spin coating of 3 wt % solutions of the functionalized PSU in cyclohexanone directly onto the polyamide disk. This procedure could be used as the PA is not swollen by the cyclohexanone. The thickness of films prepared on a silicon wafer under identical conditions was measured by AFM and was $\sim$ 250 nm for all reactive polymers. The coated PA disks and the PSU disks were dried separately at 40°C for 24 h in vacuum prior to further thermal annealing. The PSU and the coated PA disks were then brought into contact so that the spin-coated film was located in the middle of the two polymers. These specimens were placed into a hot press. To achieve intimate contact between the two disks, slight pressure was applied. The samples were always isothermally annealed in the hot press at 215°C, well above the glass transitions of the PSU and the PA, but still below the melting point of the PA, as it was a temperature that could be sustained for a longer time period by the PA without any substantial degradation. Also, the dimensions of the specimens did not change. Using thin films of reactive PSUs in sandwich specimens was necessary because only small amounts of these materials were available. Thus the reinforcement of the interface is not only a matter of reaction kinetics but it is also influenced by diffusion kinetics, as will be outlined below.

Fracture Toughness Test

After annealing for different periods of time, the joint specimens were cut into strips of 5×50 mm in length. The sample was fractured using an asymmetric double cantilever beam (ADCB) test. To make the sample asymmetric, the PA side was always glued onto a glass plate. A double-edged razor blade was inserted at the interface and pushed slowly into the sample until the crack started to propagate into the nonfractured interfacial region. Then the razor blade was not pushed anymore and the length of the crack was allowed to reach a constant value. The crack length, a, was measured under a light microscope (Olympus Vanox AH2 Research Microscope). This procedure was repeated several times for each fracture test specimen and at least five specimens were employed. Using the thickness of the PSU plates, d, and the Young modulus, E, of the PSU, values of the fracture toughness, G_c (fracture energy per unit area), were evaluated by the relation[5]

$$G_c = \frac{3Ed^3b^2}{8a^4\left[1 + \left(0.64\,\frac{d}{a}\right)\right]^4} \qquad (1)$$

where $E(\mathrm{PSU}) = 2600$ MPa.[13] A typical data set at a certain annealing time consisted of $\sim$ 15–20 measurements for each sample. In order to determine the contribution of G_c which is due to pure interfacial adhesion, the nonreactive system, just consisting of a PA/PSU joint specimen, was treated and annealed under the same conditions as described for the reactive systems. An asymmetric test geometry was also used by other groups for reactive systems.[14–17] The main reason to use this asymmetric test is to prevent crazing, which appears in symmetric samples when the more compliant material also has a lower crazing stress than the other one.[18]

Atomic Force Microscopy (AFM)

The topography of the polymeric surfaces after the fracture test was studied with an atomic force microscope in the tapping mode (Nanoscope III, Digital). Standard silicon tapping mode cantilevers were used. The smallest force was always applied in order not to alter the fracture surface. The images were treated with standard planefit and flatten procedures without applying any filters. Detailed information about AFM on polymer surfaces may be found elsewhere.[19,20]

X-ray Photoelectron Spectroscopy (XPS)

The surface chemical composition of the as-received polymers and of the fracture surfaces was

measured by XPS using a VG ESCALAB 5 spectrometer with nonmonochromatized MgKα (1253.6 eV) radiation emitted by a 200 W anode power. Survey spectra were taken with a 50 eV pass energy and detailed spectra with 20 eV pass energy in the constant analyzer mode. The base pressure in the spectrometer was $< 10^{-8}$ Pa. The sample charge was corrected by setting the binding energy of the hydrocarbon component of the C1s peak at 285.0 eV.[21,22] C1s peaks were fitted according to the references of pure polymers[21] with a width (FHWM) of 1.7 eV and fixed binding energies. The composition of the sample was deduced from the integral of the peaks after a Shirley background substraction. For XPS measurements fractured samples at two matching pieces were taken, i.e., from the PSU and the exactly opposing PA side. The XPS spot was placed in the middle of the new fracture surface which was formed during failure.

RESULTS AND DISCUSSION

Fracture Test

Figure 1(a) shows the fracture toughness, G_c, of the systems PSU/PSU-COOH$_x$/PA with different degrees of functionality, x, plotted as a function of annealing time. For comparison, the nonreactive system PSU/PA is also depicted. In the case of the reactive systems a PSU-PA graft copolymer is formed by the interfacial reaction between the carboxylic acid groups of the copolymer and the amine endgroups of the PA. It can be seen that the fracture toughness of the reactive systems increases with reaction time significantly, whereas the nonreactive system shows a comparable small increase. The maximum G_c is reached after an annealing time of 12 h. The fracture toughness of the nonreactive system originates from pure physical adhesion. The system with the reactive compatibilizer PSU-COOH$_{8.8}$ has the most significant effect of the interfacial grafting reaction on G_c. The systems containing fewer carboxylic acid groups have slightly different characteristics. The increase of G_c is smaller and can be explained by a smaller degree of functionalization leading to a smaller number of linkage points at the interface. This effect is most pronounced for the COOH-modified PSU with a degree of functionality of 1.7. Another effect arises from the interdiffusion between the thin layer of functionalized PSU and the PSU bulk phase. The measured fracture

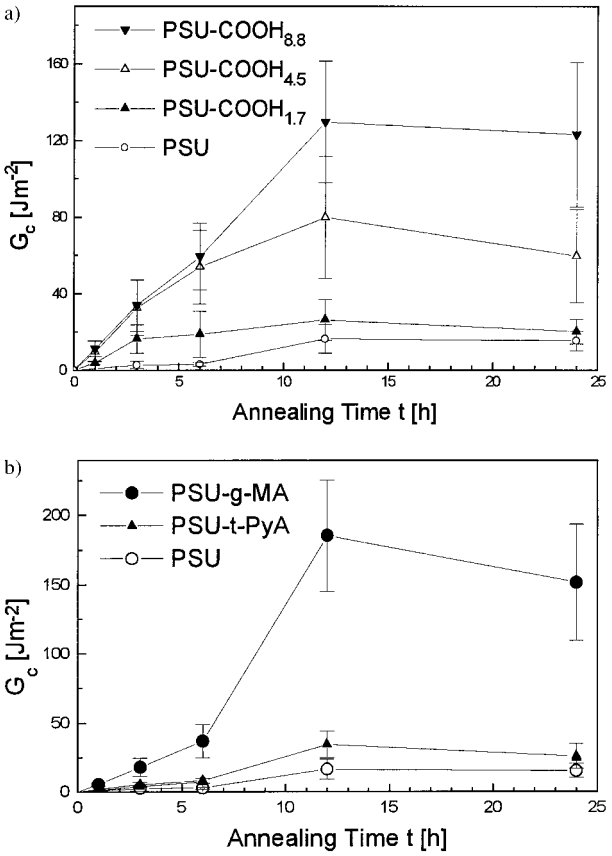

Figure 1 Fracture toughness, G_c, as a function of annealing time. The open circles represent the nonreactive system. (a) PSU/PSU-COOH$_x$/PA; (b) PSU/PSU-t-PyA/PA, PSU/PSU-g-MA/PA.

toughness is therefore a result of two separate effects, namely the reaction rate of amine endgroups of the PA with carboxylic acid groups of the PSU and the decrease of the concentration of reactive groups by interdiffusion. The diffusion coefficients of the functionalized PSUs used were determined by nuclear reaction analysis.[23] It was found that PSU-COOH$_{1.7}$ and PSU-COOH$_{4.5}$ have approximately the same diffusion coefficient of 0.91×10^{-14} and 0.96×10^{-14} cm^2 s^{-1} (at 190°C), respectively, whereas PSU-COOH$_{8.8}$ is only partially miscible with PSU. As already discussed, G_c increases with the amount of carboxylic acid groups for a comparable annealing time. Thus it can be concluded that G_c is a function of the degree of functionality, x, especially for the systems PSU-COOH$_{1.7}$ and PSU-COOH$_{4.5}$, which have a nearly identical diffusion coefficient. The system PSU-COOH$_{8.8}$ with a higher COOH-content does also fit into this tendency. All investigated systems reach their highest fracture toughness after 12 h

and show a slight decrease in G_c for an annealing time of 24 h. This can be explained by XPS measurements and will be discussed in detail below. Figure 1(b) shows the fracture toughness versus annealing time of the PSU/PSU-g-MA/PA and the PSU/PSU-t-PyA/PA system isothermally annealed at 215°C (the nonreactive system is added for comparison). It can be seen that the fracture toughness of PSU/PSU-g-MA/PA increases with reaction time significantly, whereas the system PSU/PSU-t-PyA/PA shows a comparable small increase. PSU-g-MA has a significantly smaller diffusion coefficient with PSU (0.17×10^{-14} cm^2 s^{-1}) compared to the other systems under investigation due to a lower mobility caused by a higher molecular weight and T_g. The small diffusion coefficient implies that PSU-g-MA is significantly longer present directly at the PSU/PA interface compared to the other systems. Furthermore, it is well established that anhydride groups are more reactive with amine groups than carboxylic acid groups. Therefore, it can be concluded that the high fracture toughness in the system PSU/PSU-g-MA/PA might be caused by the faster reaction rate between the reactive components and simultaneously by the slow diffusion of PSU-g-MA into the PSU bulk phase.

According to Guégan et al.[24] an increased reaction rate can be expected for reactions at polymer interfaces compared to polmer-polymer reactions in the homogeneous state, as the chain ends are enriched at polymer interfaces. Therefore, the pyromellitic anhydride endgroups of PSU-t-PyA should be enriched at the interface and highly accessible for amine endgroups of PA, which again are enriched at the polymer interface. This would lead to the assumption that a high concentration of functional groups is present at the PSU-t-PyA/PA interface, and high reaction rates and eventually high conversions can be expected. Therefore, high values for the interfacial fracture toughness should result. However, this system has very low G_c values, as can be seen in Figure 1(b). These comparable small values are reached despite the fact that the diffusion coefficient is similar to that of the carboxylic acid functionalized systems (1.11×10^{-14} cm^2 s^{-1}).

The fracture toughness at the interface is increased significantly by the chemical reaction between functionalized PSUs and PA at the polymer interface compared to the nonreactive system PSU/PA. This is observed for all reactive compatibilizers. With increasing annealing or reaction time, the fracture toughness rises considerably and reaches always its maximum value after 12 h. In Table II the maximum values of G_c are shown for all systems, i.e., the reactive and the nonreactive systems, after an annealing time of 12 h. The maximum increase of the fracture toughness at the interface, i.e., the difference between the nonreactive system and the system PSU/PSU-t-PyA/PA, is only 18 J m^{-2}. In the other systems graft copolymers are formed during the chemical reaction. With increasing COOH-content the maximum G_c is almost increasing linearly in the systems PSU/PSU-COOH$_x$/PA and a maximum G_c of 130.2 J m^{-2} is achieved. However, the best improvement in G_c is achieved in the system PSU/PSU-g-MA/PA, where G_c reaches a maximum value of 185 J m^{-2} after an annealing time of 12 h. Thus it is possible to obtain samples with a broad range of interfacial toughness in order to study details of the PSU/PA interface reinforced by chemical reaction.

Table II Maximum G_c of the Systems PSU/PSU$_x$/PA Under Investigation

PSU/PSU$_x$/PA	Maximum G_c (J m^{-2})
PSU	16.3
PSU-t-PyA	34.3
PSU-COOH$_{1.7}$	26.2
PSU-COOH$_{4.5}$	79.8
PSU-COOH$_{8.8}$	130.2
PSU-g-MA	185.2

t = 12 h, T = 215°C.

Crack Opening Geometry

The crack opening geometry can be evaluated quantitatively by interference light microscopy.[25,26] Figure 2 shows an interference light micrograph obtained for the system PSU/PSU-COOH$_{1.7}$/PA after an annealing time of 12 h. A typical interference pattern of converging lines at the crack tip can be observed. According to Döll[25] and Döll and Könczöl[26] the occurrence of this pattern can be seen when i) the material is transparent, ii) the crack opening displacement is at least in the order of magnitude of the wavelength of the applied light, and iii) the surfaces at the crack opening are smooth and well-defined and the refractive index differences at the reflecting surfaces are large enough, as it is the case for polymer/air.

If there is a craze zone in front of the crack tip,

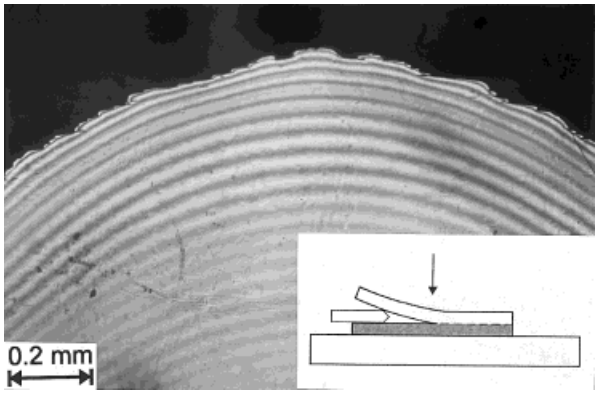

Figure 2 Interference light micrograph of the crack tip for the system PSU/PSU-COOH$_{1.7}$/PA after an annealing time of 12 h. The arrow in the inset indicates the crack tip from where the photograph is taken.

two bands of converging interference lines appear, which meet at the crack tip.[18] This can generally not be observed for the systems under discussion. This might be caused either by the fact that crazing does not appear or that the crazes have dimensions much smaller than the wavelength of the light used. It is also found that the interference pattern occurs only for relatively weak interfaces ($\sim G_c < 40$ J m^{-2}). At higher fracture toughness the surfaces are plastically deformed, and thus requirements for interference are not met anymore. This will be discussed in detail below. Using the interference theory[25] it is possible to calculate the crack opening geometry from the interference pattern. Eqs. (2) give the relation for the calculation of the crack opening, 2ν, as a function of the distance from the crack tip, y

$$2\nu(y) = \frac{\lambda}{2\mu}\left(n - \frac{1}{2}\right) \quad 2\nu(y) = \frac{\lambda}{2\mu}n$$

$$n = 1, 2, 3, \ldots \quad (2)$$

where λ is the wavelength of the light ($\sim$ 600 nm), μ is the refractive index of air ($\mu = 1$), and n is the order of the interference fringe. The left equation is for positive interference, the other equation for negative interference. It should be mentioned that the first interference fringe is assigned to $n = 1$. In the case that the crack tip has already a large opening, the first visible interference fringe might be already of higher order. This would result in a shift of the crack opening displacement toward higher y values, while the opening geometry is described consistently. Figure 3 depicts the crack opening geometry for the system PSU/PSU-COOH$_{1.7}$/PA after different annealing times. The opening geometry after 12 h of annealing is obtained using the photograph shown in Figure 2. All crack opening geometries have a more parabola-like shape close to the crack tip. With increasing distance from the crack tip the geometry changes to a hyperbolic form. Because of the increase of $2\nu(y)$ with increasing annealing times, it can be concluded that the stress absorption at the crack tip improves with longer annealing times. This is synonymous with the formation of more chemical bonds across the interface, and thus related to the increase of G_c.

Examination of the Fracture Surface

Light Microscopy Measurements

The fracture surfaces on both sides of the failed interface are studied by light microscopy (LM) and atomic force microscopy (AFM). The micrographs shown in Figure 4(a,b) are obtained by reflection light microscopy. They are taken at exactly opposing sides of failed fracture surfaces of the system PSU/PSU-g-MA/PA after an annealing time of 12 h. This system is chosen because it has the highest G_c value. In order to obtain these micrographs the sample is completely separated after reaching its equilibrium crack length, and the former arrested crack tip is indicated by arrows on both sides. The artifact at the lower part of the photographs is shown in order to make

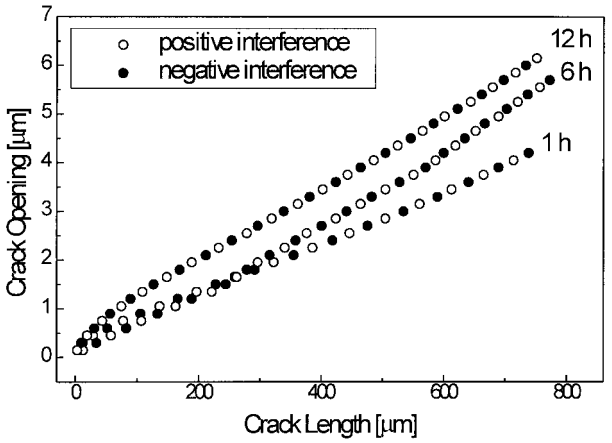

Figure 3 Crack opening geometries after different annealing times for the system PSU/PSU-COOH$_{1.7}$/PA. (●), negative interference; (○), positive interference.

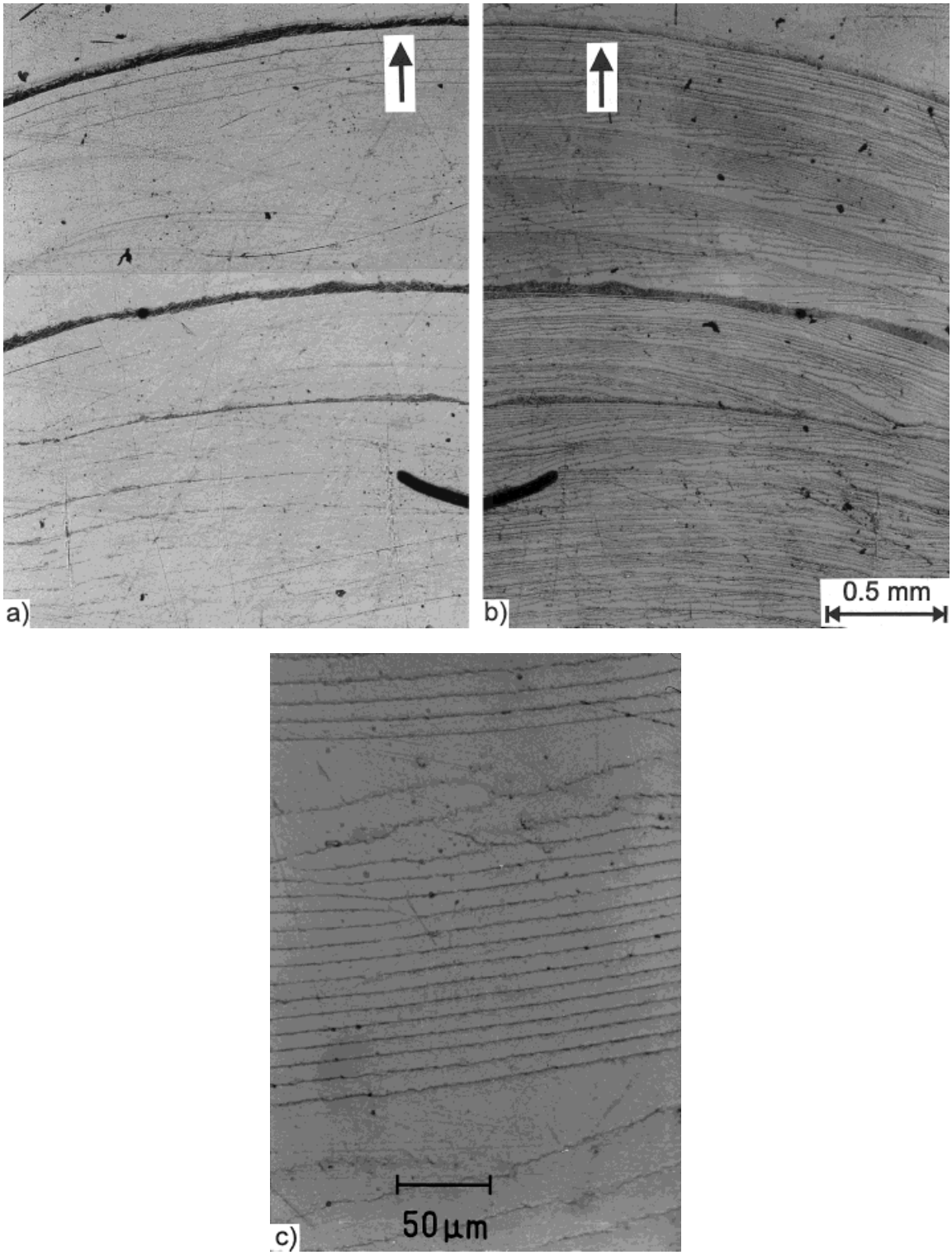

Figure 4 Reflection light micrographs of the fracture surfaces of the system PSU/PSU-g-MA/PA after annealing for 12 h at 215°C. (a) PA surface; (b) PSU surface. The direction of crack propagation is from bottom to top. (c) as (b), but enlarged; the crack propagation direction is from top to bottom.

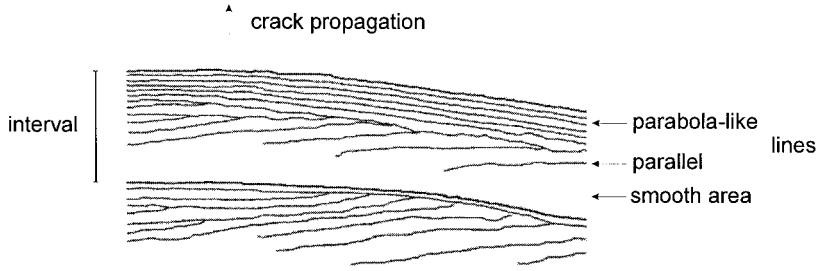

Figure 5 Schematic representation of the morphology of the PSU fracture surface after failure, according to Figure 4(b).

sure that exactly the complementary fracture surfaces are probed. On the PA side only a few traces are identified, whereas on the PSU side a regular pattern can be observed. Behind the crack tip, parallel parabola-like lines perpendicular to the crack propagation direction which occur quite regularly are visible. Repeating units of these lines consist of a rough and a fine structure and occur quite regularly. The fracture surface of PSU shows more lines caused by plastic deformation than the fracture surface of PA. The most pronounced lines can be seen on both sides of the failed interface and appear exactly complementary. Figure 4(c) shows the PSU fracture surface with a higher magnification. The rib marking-like lines have a substructure which appears wound. The bright spots on the rib marking lines are deformed material which is elongated during the fracture process. The surface morphology of the failed PSU side is schematically shown in Figure 5. Behind the crack tip, parallel parabola-like lines perpendicular to the crack propagation direction which occur quite regularly can be identified. The width of the intervals decreases toward the crack tip. These intervals start with a smooth unstructured surface which is followed by a bunch of lines which are almost perpendicular to the crack propagation direction. They are followed by a group of parabola-like lines which are equidistant. The whole appearance of the surface morphology can be explained using a slip-stick-like crack propagation mechanism. The jerky crack propagation can also be observed in the light microscope, i.e., the crack jumps from one rib marking line to the next. The smooth start of the intervals is a result of the relatively fast crack propagation. Then the crack propagation slows down and stops. This is connected with a build-up of a stress which is released after reaching a critical value. Caused by the coupling reaction between the anhydride and carboxylic acid-modified PSUs, respectively, and the PA at the interface, a polymer with an anchor function is formed which is capable of reinforcing the originally weak PSU/PA interface. Thus the chemical reaction reinforces the interface to such a level that not only adhesive failure at the interface occurs but the level of cohesive failure of the bulk materials is reached.

AFM Measurements

To get more detailed information about the PSU fracture surfaces, AFM measurements of specimens with different annealing times were carried out. Figure 6(a,b) show tapping mode AFM measurements of the PSU fracture surface after 6 and 12 h of annealing at 215°C, respectively. It is clear that the failure mechanism changes for different annealing times. The specimen after an annealing time of 6 h has more and less deformed areas uniformly distributed over the whole fracture surface [Fig. 6(a)]. Lines are arranged relatively parallel and perpendicular to the crack propagation direction, but they have branching points, which means that the lines are partially connected. Thus it can be concluded that the stress at the crack tip is released continuously during propagation. The fracture seems not to occur in regular steps at the whole crack front, but the failure occurs continuously at different spots during the crack propagation. This is caused by the less reinforced interface after an annealing time of 6 h compared to longer annealing times. Figure 6(b) depicts regular and well-defined lines perpendicular to the crack propagation direction. As has been described in Figure 5, the sample annealed for 12 h shows a regular pattern of intervals consisting of three major regions. The AFM measurements are done in the area of the parabola-like regular lines. The measured lines correspond to the former propagation front and represent the location where the interface has be-

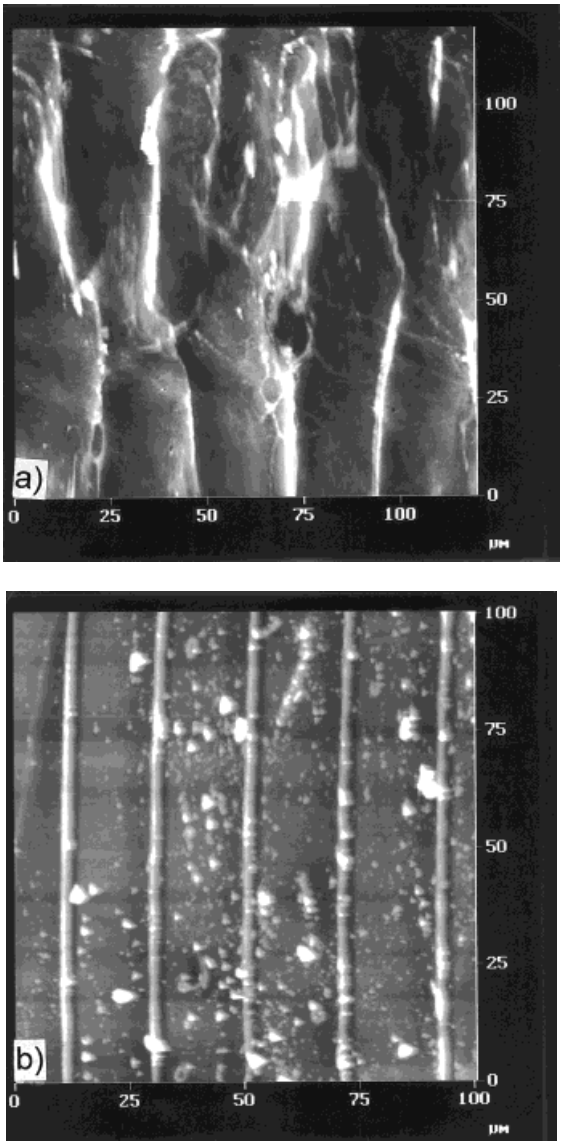

Figure 6 AFM micrographs of PSU fracture surfaces after annealing times of (a) 6 h and (b) 12 h at 215°C for the system PSU/PSU-g-MA/PA. The direction of the crack propagation is from the left to the right.

gun to fail in response to the applied load. The fracture occurs in regular steps (slip-stick mechanism) at the whole crack front that correspond to these rib marking-like lines. On these lines hillocks are visible (bright dots). These lines are ~ 300–400 nm high and the distance to another line is ~ 20–30 μm.

XPS Measurements

In order to prove the interfacial reaction between functionalized PSU and PA, a direct method such as FTIR can not be used because the signal-to-noise ratio is too poor for the detection of an interfacial reaction in samples with such a small concentration of reactive groups.[27] A PA disk is coated with a 250-nm thick layer of PSU-g-MA and the coated sample is annealed at 215°C for 3 h. After removing the nonreacted PSU-g-MA by extraction with tetrahydrofuran, the remaining PSU grafted onto PA is detected by XPS. Besides carbon, nitrogen, and oxygen, it is possible to detect sulfur, which belongs definitively to PSU covalently bonded to PA.

To determine the mode of failure of the PSU/PSU-g-MA/PA system, PSU and PA fracture surfaces—obtained after different annealing times at 215°C—are analyzed by XPS. The as-received PSU and PA surfaces are also analyzed and are taken as references for the chemical composition of each polymer and for the fit of the C1s peak. On both sides of the fracture surfaces, traces of silicon are detected. The PSU composition corresponds well to the theoretical values, but the PA nitrogen content (7.5 at. %) is found to be far smaller than the value calculated from the structural unit of the polymer (11.5 at. %). This difference was also reported for other commercial polyamides.[28]

Figure 7 shows N1s and S2p XPS detailed spectra of the PSU fracture surfaces of the system PSU/PSU-g-MA/PA annealed for different times at 215°C. It can be seen that the nitrogen content of the PSU fracture surface increases continuously with longer annealing times [Fig. 7(a)] and reaches 5.5 at. % after 24 h of annealing. Complementary to the nitrogen content on the PSU fracture surface, the sulfur content decreases continuously, to be almost zero after 24 h of annealing [Fig. 7(b)]. The intensity of the nitrogen peak can be directly related to the amount of PA on the PSU surface, because only the PA contains nitrogen. Therefore, the amount of PA on the PSU fracture surface increases continuously with annealing time. On the contrary, it is impossible to detect any amount of sulfur on the fracture surface of the PA side, i.e., PSU is not present on the PA surface after the fracture. Therefore, the failure of this sample is mainly of cohesive nature, i.e., the system does not fail at the interface, but in the PA material. With increasing annealing time the chemical reaction between the PSU-g-MA and the PA becomes more completely achieved and the sample tends to fail more and more in the PA phase during the fracture test. This proves the efficiency of the chemical reaction

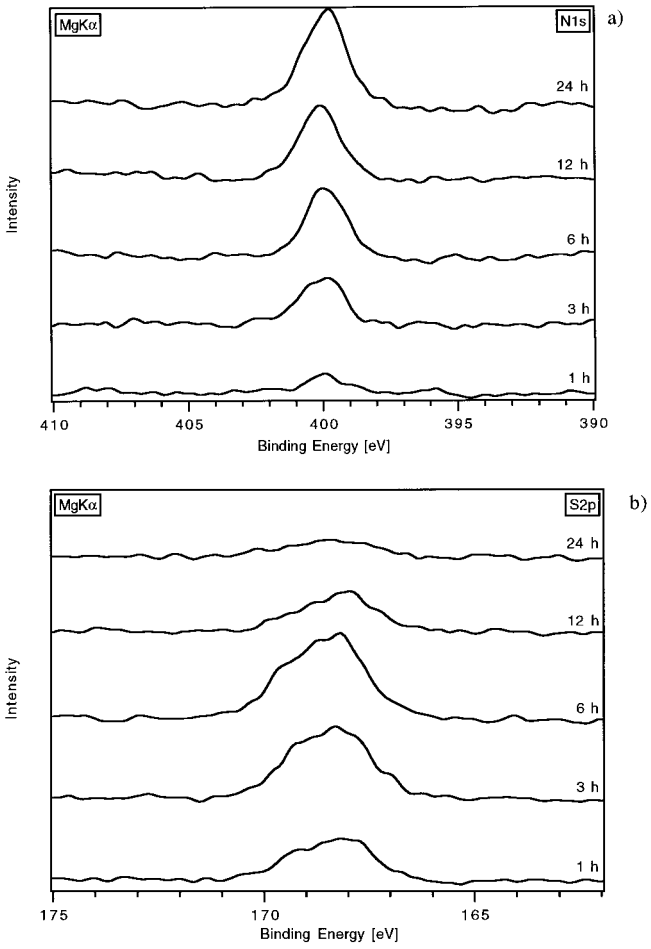

Figure 7 XPS spectra of the fracture surface of the PSU side of the system PSU/PSU-g-MA/PA after different annealing times at 215°C: (a) nitrogen N1s; (b) sulfur S2p.

induced by the addition of PSU-g-MA at the interface.

The cohesive fracture process can be confirmed by fitting the C1s peak of the PSU [Fig. 8(a)] and of the PA [Fig. 8(b)] fracture surfaces of PSU/PSU-g-MA/PA after different annealing times. According to the references of PSU and PA XPS measurements[22] and to the fit of the as-received surfaces, the measured C1s peak (dotted line) of the PSU fracture surface can be fitted with two peaks for the as-received sample, with three or four peaks for the annealed samples. The signal of the aromatic and aliphatic carbon atoms (E = 285.0 eV) is taken as reference to correct the spectra for the charging effect. The ether carbon (C—O—C) has a shift of ΔE = 1.45 eV, and the amide carbon (CONH) has a shift of ΔE = 2.9 eV. As it can be seen in Figure 8(a), the C1s peak has increasing contributions of signals at higher binding energies with increasing annealing time. Already after an annealing time of 1 h, the peak

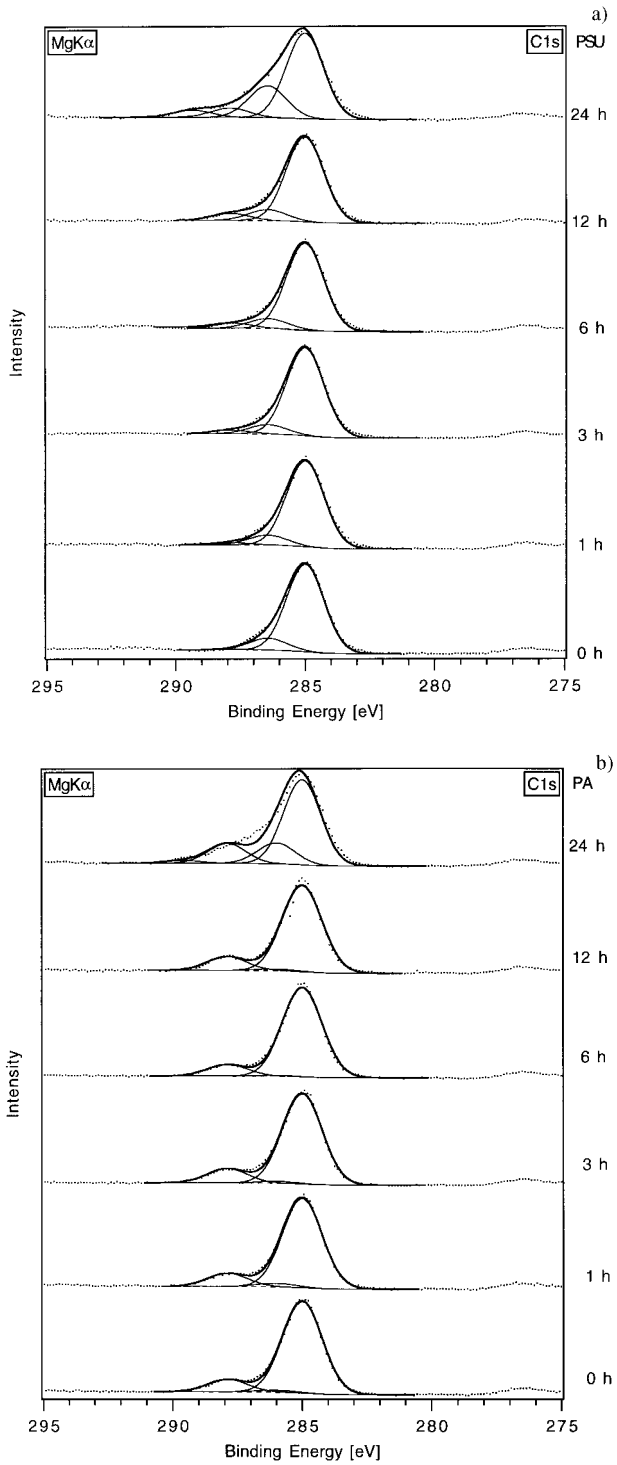

Figure 8 C1s XPS spectra of the fracture surfaces of the system PSU/PSU-g-MA/PA isothermally annealed at 215°C for different times: (a) PSU side; (b) PA side.

Table III Content of Nitrogen and Amide Carbon (CONH) on the PSU Side of the System PSU/PSU-g-MA/PA after Different Annealing Times at 215°C, and Calculated Amount of Cohesive Failure

t (h)	Nitrogen (at. %)	Cohesive Failure (%)	CONH (at. %)	Cohesive Failure (%)
0	0	—	0.6[a]	—
1	2.1	28.0	2.1	20.0
3	3.3	44.0	3.5	33.3
6	4.1	54.7	4.2	40.0
12	5.2	69.3	6.7	63.8
24	5.5	73.3	6.9	65.7
PA (as received)	7.5	—	10.5	—

[a] Originates from fitting procedure.

corresponding to amide carbon is visible. This signal stems from the failed PA on the PSU fracture surface. This signal increases continuously with increasing annealing time, reflecting the increasing amount of PA on the PSU side.

The C1s XPS spectra of the PA fracture surface of PSU/PSU-g-MA/PA [Fig. 8(b)] are fitted with three or four peaks, depending on the annealing time. The α-carbon next to the nitrogen of the amide group (— $C_\alpha H_2$ — NH —) is fitted with a energy shift of ΔE = 1 eV, and the amide carbon (CONH) with ΔE = 2.9 eV. These three signals remain approximately constant for all fits up to 12 h. Therefore, the fits of the C1s peaks confirm that the fracture is mainly of cohesive nature, and thus occurs into the PA side. Moreover, cohesive failure of the PSU can be excluded.

It is clear that the failure mechanism changes from adhesive failure at the weak interface (PSU/PA system) to dominant cohesive failure in the PA bulk phase when the interface is sufficiently reinforced by the chemical reaction. Taking into account the amount of nitrogen and the contribution of the amide carbon atoms in the C1s peak measured on the PSU fracture surface (Table III), it is possible to estimate the ratio of adhesive failure to cohesive failure. In the case of sole cohesive failure, e.g., of sole failure in the PA phase, the amount of nitrogen found on the fracture surface of PSU must be equal to that of the PA bulk phase. This assumption holds only when the fracture surface is covered with a homogeneous layer > 5 nm because the depth probed by XPS measurements is in this range.[22] This assumption is reasonable because the radius of gyration of polymers has approximately the same dimension. To calculate the values in Table III, it is assumed that 100% cohesive failure means that the nitrogen content of the PSU fracture surface is equal to that of the PA phase (7.5 at. %), or that the amount of detected amide carbon on the PSU fracture surface equals the amount of amide carbon in the PA phase (10.5%). It has to be mentioned firstly, that the percentage of the amide carbon originates from a fit which leads to a larger error in the further calculation and, secondly, that the small amount of amide carbon on the PSU surface after an annealing time of 0 h is caused by the fitting procedure and is not significant. Once again, it is obvious that the percentage of cohesive failure in the PA phase increases steadily with increasing annealing times, and reaches a plateau value of $\sim$ 70%. This plateau occurs after 12 h of annealing, which corresponds to the point where the limit of G_c is reached.

Similar behavior, namely partially cohesive failure in one of the materials, has been observed for several other systems such as polystyrene/polystyrene-block-poly(methyl methacrylate)/poly(methyl methacrylate) (PS/PS-b-PMMA/PMMA), poly(styrene-co-acrylonitrile)/PMMA, and poly(styrene-co-acrylonitrile)/polycarbonate.[29–32] For all these systems, a cohesive fracture occurs to some extent in the most compliant polymer or in the polymer with the lower entanglement density and lower craze stress.

The fits of the C1s peaks are also able to provide a reasonable explanation of the small decrease of the fracture toughness for annealing times longer than 12 h. As it can be observed in Figure 8, an additional peak is necessary to fit the measured data of both sides of the fracture after an annealing of 24 h. The shift of the binding energy is found to be $\sim$ ΔE = 4 eV. It seems reasonable that during the degradation process of polyamides free carboxylic acid groups are formed. Therefore, this additional peak can be attributed to the signal of COOH. This peak occurs exclusively at an-

nealing times of 24 h. Moreover, it is obvious from Figure 8(b) that the C1s peak of the PA fracture surface after annealing for 24 h needs an additional peak at $\sim$ 287 eV to be correctly fitted. The degradation process of the PA seems also to induce several new oxidation states of the polymer. Therefore, it can be assumed that the small decrease of the fracture toughness for annealing times $>$ 12 h for all systems under investigation is caused by the oxidation (degradation) process of the polyamide.

CONCLUSIONS

The weak interface between PSU and PA can significantly be reinforced by the chemical reaction between amine groups of the PA and anhydride or carboxylic acid groups of modified PSUs. The efficiency of the PSU-$COOH_x$ as a compatibilization agent is dependent on the degree of functionality. A change in failure mechanism can be observed for weakly and strongly reinforced interfaces as shown by LM and AFM. XPS measurements indicate that the failure during the fracture test occurs more and more in the PA bulk phase. There is a shift from mainly adhesive failure in weak interfaces to dominant cohesive failure in the PA bulk phase for strongly reinforced interfaces.

REFERENCES

1. A. Utracki and A. Leszek, *Polymer Alloys and Blends,* Hanser Pub., Munich, 1989.
2. R. Fayt, R. Jérôme, and P. J. Teyssié, *J. Polym. Sci., Polym. Phys. Ed.,* **20,** 2209 (1982).
3. C. R. Lindsey, D. R. Paul, and J. W. Barlow, *J. Appl. Polym. Sci.,* **26,** 1 (1981).
4. M. Xanthos, *Reactive Extrusion,* Hanser Pub., Munich, 1992.
5. H. R. Brown, *J. Mater. Sci.,* **25,** 2791 (1990).
6. H.-H. Hub, G. Blinne, H. Reimann, P. Neumann, and G. Schaefer, Ger. Pat. DE-Pat. 34 44 339, (1984).
7. I. C. H. M. Esser and I. W. Parsons, *Polymer,* **34,** 2836 (1993).
8. T. Koch and H. Ritter, *Macromol. Chem. Phys.,* **195,** 1709 (1994).
9. M. Weber and K. Mühlbach, Ger. Pat. DE-A 41 10 460, (1991).
10. C. L. Myers, *SPE Conference Proceedings of ANTEC,* Detroit, **1,** 1420 (1992).
11. S. Wu, *Polymer,* **29,** 229 (1992).
12. J. H. Kawakami, C. T. Kwiatkowski, G. L. Brode, and A. W. Bodwin, *J. Polym. Sci., Poly. Chem. Ed.,* **12,** 565 (1974).
13. BASF Ultrason® S data sheet (1992).
14. Y. Lee and K. Char, *Macromolecules,* **27,** 2603 (1994).
15. E. Boucher, J. P. Folkers, H. Hervet, L. Léger, and C. Creton, *Macromolecules,* **29,** 774 (1996).
16. J.-E. Bidaux, G. D. Smith, N. Bernet, J.-A. E. Månson, and J. Hilborn, *Polymer,* **37,** 1129 (1996).
17. N. C. Beck Tan, S.-K. Tai, and R. M. Briber, *Polymer,* **37,** 3509 (1996).
18. C. Creton, E. J. Kramer, C.-Y. Hui, and H. R. Brown, *Macromolecules,* **25,** 3075 (1992).
19. V. V. Tsukruk and D. H. Reneker, *Polymer,* **36,** 1791 (1995).
20. M. Radmacher, R. W. Tillmann, M. Fritz, and H. E. Gaub, *Science,* **257,** 1900 (1992).
21. G. Beamson and D. Briggs, *High Resolution XPS of Organic Polymers,* Wiley, New York, 1992.
22. D. Briggs and M. D. Seah, Eds., *Practical Surface Analysis,* Wiley, New York, 1993.
23. W. Straub, M. Collaud Coen, D. Mäder, J. Kressler, and R. Brenn, *J. Polym. Sci., Polym. Phys.,* submitted.
24. P. Guégan, C. W. Macosko, T. Ishizone, A. Hirao, and S. Nakhama, *Macromolecules,* **27,** 4993 (1994).
25. W. Döll, *Adv. Polym. Sci.,* 52/53, Springer, Berlin, 1983.
26. W. Döll and L. Könczöl, *Adv. Polym. Sci.,* 91/92, Springer, Berlin, 1991.
27. D. Mäder, J. Kressler, and M. Weber, *Macromol. Symp.,* **112,** 123 (1996).
28. M. Collaud Coen, M. Pisinger, S. Nowak, F. Stucki, and L. Schlapbach, *J. Adhesion,* **53,** 201 (1995).
29. K. Cho, H. R. Brown, and D. C. Miller, *J. Polym. Sci., Polym. Phys. Ed.,* **28,** 1699 (1990).
30. K. L. Foster and R. P. Wool, *Macromolecules,* **24,** 1397 (1991).
31. J. L. Willett and R. P. Wool, *Macromolecules,* **26,** 5336 (1993).
32. R. P. Wool, *Polymer Interfaces, Structure and Strength,* Hanser Pub., Munich, 1995.